The anisotropy of metals is an important property that has a significant impact on the dimensional accuracy of components in manufacturing. In metal forming processes significant attention has been given to multilayer composite sheets as they may combine the advantages of materials with various mechanical properties. In this study, the effect of anisotropy is investigated in the process of single point incremental forming (SPIF) of aluminum bilayer sheets. The finite element method (FEM) is used to study the effect of layer arrangement and the anisotropy of metal sheets relative to the rolling direction. For the effective description of sheet metal anisotropy, the two-dimensional Yld2000-2D yield function is implemented in Abaqus software using a material subroutine (VUMAT). The calculation and calibration of the coefficients of Yld2000-2D in accordance with the experimental data were performed using a MATLAB code. For comparison, the anisotropic coefficients of Yld2000-2D were replaced by unit values in the same VUMAT to investigate forming behavior in the isotropic case with the von Mises yield function. Anisotropic and isotropic models are compared in a conical geometry by assessing equivalent plastic strain, sheet thickness, and forming tool reaction forces. Our findings show that anisotropy of sheet metal causes less variation in material properties compared to the isotropic case, significantly affecting the stiffness and, subsequently, the final shape dimensional accuracy of the formed component. The results of the study have a practical application in that they can be used to identify strategies for anisotropic bimetal sheets to improve such material forming processes

Keywords: anisotropy, incremental metal forming, aluminum alloys, bilayer sheet, finite element analysis, Yld2000-2D

UDC 621
DOI: 10.15587/1729-4061.2022.256225

NUMERICAL STUDY ON THE EFFECT OF ANISOTROPY ON DEFORMATION BEHAVIOR OF ALUMINUM BILAYER SHEETS IN SINGLE POINT INCREMENTAL METAL FORMING

Bassam Abdullah Mohammed
Corresponding author
Doctor of Mechanical Engineering*
E-mail: bassam.moh@stu.edu.iq
Raed Sabri Batbooti
Doctor of Mechanical Engineering*
Tahseen Ali Jabbar
Doctor of Mechanical Engineering*
*Basra Engineering Technical College
Southern Technical University
Al-Zubair str., Basra, Iraq, 61003

Received date 05.04.2022
Accepted date 06.06.2022
Published date 30.06.2022

How to Cite: *Mohammed, B. A., Batbooti, R. S., Jabbar, T. A. (2022). Numerical study on the effect of anisotropy on deformation behavior of aluminum bilayer sheets in single point incremental metal forming. Eastern-European Journal of Enterprise Technologies, 3 (1 (117)), 50–57. doi: https://doi.org/10.15587/1729-4061.2022.256225*

1. Introduction

Increased demand for economical methods of manufacturing has led to the development and implementation of many new techniques, such as incremental sheet metal forming (ISMF). With ISMF, complex sheet metal parts can be fabricated without using dies or specific tools. In ISMF, a fixed sheet is formed into a particular shape by using a hemispherical tool with a predefined path. Two-point incremental forming (TPIF) and single-point incremental forming (SPIF) are the most widely used ISMF procedures. The primary difference between them is that there is a die under the formed sheet in TPIF but not in SPIF [1]. The parameters that affect ISMF include sheet thickness, wall angle, feed rate, tool geometry, tool rotational speed, tool step depth, and sheet arrangement for multilayer sheets [2].

The laminate composites of metals with various properties have important industrial applications. In the electromechanical industry, the fact that there are numerous uses for dissimilar metal sheets manufactured by roll bonding or explosive welding can be attributed to their superior inclusive properties. They take the benefits of incorporating physical and mechanical characteristics from various base materials. Therefore, studies that are devoted to examining the formability of anisotropic bilayer sheets in SPIF by constructing a finite element model and analyzing the mechanical features of the formed parts based on an advanced anisotropic material yield model are of scientific relevance.

2. Literature review and problem statement

Most ISMF studies and review papers consider single-layer sheet metals exhibiting isotropic behavior. However, too little effort has been devoted to predicting the effect of anisotropy in single-layer metal sheets using SPIF. The effect of anisotropy was investigated in magnesium alloy AZ31 sheets at high temperatures using SPIF in [3]. The researchers concluded that sheet anisotropy has an important impact on the quality of the surface and the formability of parts

shaped by SPIF and that this impact turns out to be less pronounced with increasing temperature. The study [4] examined the effects of draw angle and the ratio of tool diameter to pitch for an automotive component fabricated from anisotropic titanium alloy sheets using SPIF. The authors showed that a high tool diameter to pitch ratio results in uniform thickness distribution and enhances the surface finish. The stress-based forming limit of AA6022 alloy sheets was utilized to study the necking phenomenon in SPIF [5]. The finite element (FE) analysis with anisotropic Hill48 yield criterion was used to simulate truncated pyramid geometry. The authors concluded that the stress states on the surfaces of the simulated single-layer sheet did not reach the limits of forming curve simultaneously. Moreover, each layer was shown to have various states of stress depending on its history of deformation to suppress necking.

In recent years, much has been done to examine the properties of bimetal sheets formed through such conventional processes as deep drawing or stamping. Researchers have, for instance, increasingly attended to the isotropic behavior of bimetal sheets produced through different forming procedures [6]. However, the development of structures composed of bimetal sheets with different physical properties requires a thorough familiarity with their performance. The effect of anisotropy in bimetal sheets has been the subject of much research. The study [7] experimentally investigated the effect of the anisotropy of specimens made from aluminum/copper (Al/Cu) sheets fabricated by a rolling process. Less attention has been devoted to the behavior of plastic anisotropy caused by the textures and mechanical properties of bimetal sheets in the forming processes. The texture evolution of Al/Cu sheet and the effect of plastic anisotropy on earing behavior in a deep drawing process were investigated in [8]. Researchers concluded that the mismatch between sheets of Cu and Al, particularly regarding plastic anisotropy, had a good impact on the properties of the resulting bimetal Al/Cu sheet. The FE method was used by [9] for simulating the deep drawing process of aluminum/steel (Al/St) bimetal sheets using the commercial code Abaqus with Hill48 yield function. Successful forming of a bimetallic Al/St sheet was predicted by the anisotropic FE model. They demonstrated that a wider working zone can be accomplished by a reduction in the drawing ratio, by a decrease in the thickness of the bimetal sheets with lower strength metals, and by maintaining contact between the Al sheet and the punch in Al/St layer arrangements. In addition, compared to St/Al layer arrangements, a higher drawing ratio and a thinning of the low strength Al sheet were achieved with Al/St layer arrangements.

Recently, there has been a good deal of research into the behavior of bimetal sheets during the SPIF process. A comprehensive study of the formability of Al/Cu bimetal sheets with various layer arrangements was introduced in [2]. The researchers in this study experimentally and numerically based on the isotropic plastic behavior of metal sheets investigated the effects of layer arrangements on thickness variation, forming force, and surface roughness. They found a higher forming force in the Al/Cu layer arrangement relative to the Cu/Al layer arrangement, as the outer noncontact layer with the forming tool was thinner but had a higher strength Cu layer to accomplish further deformation.

The initial sheet metal used in ISMF typically features anisotropy contributing to variations in stresses, strains, and thinning, which affect the final shape of the formed component. To the best of the authors' knowledge, investigation into the effects of bimetal sheet anisotropy on components produced by SPIF is lacking in the literature.

3. The aim and objectives of the study

The main aim of the study is to investigate the effect of the material anisotropy on the deformation behavior of bilayer sheets in the SPIF procedure by using the FE method. The practical implication of the study results is to identify ways for further improvement of such material forming processes.

To achieve this aim, the following objectives were set:

– to implement a MATLAB code to calibrate the coefficients of the Yld2000-2D yield function with the experimental results;

– to construct a FE model to simulate the SPIF process of bimetal sheets with Abaqus material subroutine (VUMAT) implemented by using FORTRAN code;

– to study the impact of layer arrangement and the difference between isotropic and anisotropic cases numerically in terms of the equivalent plastic strain, thickness distribution, and reaction forces.

4. Materials and methods

4. 1. Constitutive models

4. 1. 1. von Mises isotropic yield function

The von Mises yield function [10] has been widely applied in FE simulations of sheet metal forming processes. The three-dimensional (3D) yield function can be expressed as follows:

$$\varphi\left(\sigma_{ij}\right)=\left(\sigma_{xx}-\sigma_{yy}\right)^2+\left(\sigma_{yy}-\sigma_{zz}\right)^2+$$
$$+\left(\sigma_{zz}-\sigma_{xx}\right)^2+6\left(\sigma_{xy}^2+\sigma_{yz}^2+\sigma_{zx}^2\right)=2\bar{\sigma}^2. \quad (1)$$

In (1), the yield function is expressed by the six parts of the stress tensor (σ_{ij}), which can be described on the basis of the material coordinate system, where the rolling, transverse and thickness directions of the sheet are represented by x, y and z, respectively. The term $\bar{\sigma}$ represents the yield stress to characterize the material hardening. In the case of plane stress conditions (two-dimensional, 2D), the terms $\sigma_{zz}=\sigma_{yz}=\sigma_{zx}=0$ in (1).

4. 1. 2. Yld2000-2D anisotropic yield function

In the current study, the non-quadratic plane stress yield function called Yld2000-2D [11] was adopted to describe the behavior of the plastic anisotropy of sheet metal. The yield function is defined as follows:

$$\varphi\left(\sigma\right)=\varphi'+\varphi''=2\bar{\sigma}^m, \quad (2)$$

where

$$\varphi'=\left|\tilde{X}_1'+\tilde{X}_2'\right|^m, \quad (3)$$

and

$$\varphi''=\left|2\tilde{X}_2''+\tilde{X}_1''\right|^m+\left|2\tilde{X}_1''+\tilde{X}_2''\right|^m. \quad (4)$$

The exponent (m) is a material coefficient related to the crystal structure, which is usually set to 8 for face centered

cubic (FCC) aluminum metals. Here $\tilde{X}'_n$ and $\tilde{X}''_n$ (n=1, 2) are the principal components of the deviatoric stress tensors $\tilde{x}'$ and $\tilde{x}''$, which are determined through the linear transformation of the stress tensor σ, where $\tilde{x}'=T'\sigma$ and $\tilde{x}''=T''\sigma$. The two associated linear transformations T' and T'' contain the eight independent anisotropic coefficients k_i (i=1~8), and can be expressed as follows:

$$T'=\begin{bmatrix}T'_{11}\\T'_{12}\\T'_{21}\\T'_{22}\\T'_{66}\end{bmatrix}=\begin{bmatrix}2/3 & 0 & 0\\-1/3 & 0 & 0\\0 & -1/3 & 0\\0 & 2/3 & 0\\0 & 0 & 1\end{bmatrix}\begin{bmatrix}k_1\\k_2\\k_7\end{bmatrix}, \quad (5)$$

$$T''=\begin{bmatrix}T''_{11}\\T''_{12}\\T''_{21}\\T''_{22}\\T''_{66}\end{bmatrix}=\frac{1}{9}\begin{bmatrix}-2 & 2 & 8 & -2 & 0\\1 & -4 & -4 & 4 & 0\\4 & -4 & -4 & 1 & 0\\-2 & 8 & 2 & -2 & 0\\0 & 0 & 0 & 0 & 9\end{bmatrix}\begin{bmatrix}k_3\\k_4\\k_5\\k_6\\k_8\end{bmatrix}. \quad (6)$$

The Yld2000-2D yield function can be demonstrated in isotropic conditions where unit values are assigned for all the coefficients k_i (i=1~8). The plastic strain anisotropy parameters («r-values») and yield stresses from the tensile test of the samples tested along 0°, 90° (perpendicular; TD) and 45° (diagonal; DD) relative to the rolling direction (RD) are used. In addition, to determine the coefficients of the Yld2000-2D model, the biaxial yield stress (σ_b) and biaxial r-value (r_b) are needed. The anisotropic coefficients (k_1–k_6) can be calculated by the normalized stress ratios and r-values along the RD, TD, and biaxial directions. The other two coefficients, k_7 and k_8, can be calculated by utilizing the normalized stress ratio and r-value along the DD. For the mathematical formulation of the Yld2000-2D model, the predictor-corrector scheme [12] has been utilized to derive the yield function equations for the numerical implementation with the FE method.

4. 2. Material characterization

In this work, commercial aluminum alloy sheets AA2090-T3 (AL20) and AA7075-O (AL70) were investigated. The mechanical properties of AL20 with a 1.0 mm sheet thickness have been outlined in the previous work [13], while those of AL70 with a sheet thickness of 1.27 mm have been experimentally studied in [14]. Two terms were used to characterize the type of layer arrangement. The term AL70/AL20 refers to the AL70 sheet metal in contact with the hemispherical tool, and vice versa for AL20/AL70. The elastic mechanical properties of sheets are outlined in Table 1.

Table 1

Elastic properties of AL20 [13] and AL70 [14]

Material	E, GPa	υ	ρ, kg/m^3
AL20	278.6	98.87	27.15
AL70	73.34	161.24	26.89

Eight mechanical properties are required to calculate the eight anisotropic coefficients of the yield function Yld2000-2D. Values of the normalized yield stresses (σ_0/σ_0, σ_{45}/σ_0, σ_{90}/σ_0, and σ_b/σ_0) and the plastic anisotropy strain r-values (r_0, r_{45}, r_{90} and r_b) are shown in Table 2.

Table 2

Normalized yield stress and r-values for AL20 [13] and AL70 [14]

Material	σ_0	σ_{45}	σ_{90}	σ_b	r_0	r_{45}	r_{90}	r_b
AL20	1	0.811	0.910	1.035	0.211	1.576	0.692	0.67
AL70	1	0.971	0.989	1.142	0.877	0.972	0.752	1

To find the required hardening parameters of the materials for implementation, the tensile test results along the RD of both AL20 and AL70 were assumed as the reference case for the parameter identifications of the Voce type hardening law:

$$\bar{\sigma}(\bar{\varepsilon})=\beta+\omega\exp(-\lambda\bar{\varepsilon}), \quad (7)$$

where $\bar{\sigma}$ is the flow stress and $\bar{\varepsilon}$ is the equivalent plastic strain (EPS). The Voce type hardening law parameters are β, ω and λ. These parameters can be calibrated using the least square method in the MATLAB curve fitting toolbox, which relied on the true stress and true plastic strain experimental curve from the tensile test along the RD.

4. 3. Assumptions of the numerical simulation of single point incremental forming for the bilayer sheet

A three-dimensional FE model was created to simulate the SPIF process for bilayer sheets using Abaqus software. For the parametric study, 140 mm by 140 mm meshed sheet blanks with 2.5 mm by 2.5 mm element size were considered a deformable body. Reduced integration was performed (one integration point in the plane) by using Abaqus four-node shell type S4R elements. Six integration points were assumed within the entire thickness of the bilayer sheet, with three integration points for each layer.

To simulate the roll-bonded behavior of the composite sheet, the blank sheet is divided into two layers. The mechanical properties and orientation of each sheet layer attributed to each metal were defined. Fixed boundary conditions were created over the blank edges. The forming tool with a 12 mm diameter was assumed as a rigid surface type R3D4 element. Surface-to-surface contact was established to describe the interaction between the bilayer sheet and the forming tool surfaces. Additionally, tangential behavior with penalty friction from Abaqus was adopted to model the friction behavior between the blank and the tool with a friction coefficient of 0.1.

The tool trajectory during the SPIF process was designed with MATLAB software, generating the conical geometry used in the Abaqus/Explicit simulation. The spiral tool path was defined in the x, y, and z coordinates with a wall angle of 60°, as shown in Fig. 1.

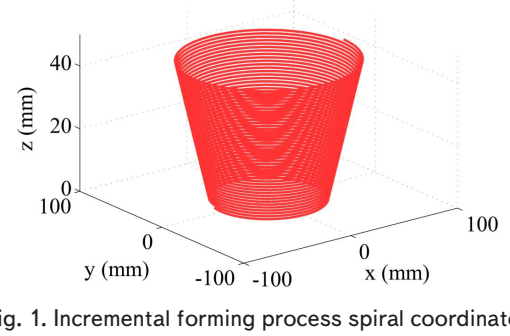

Fig. 1. Incremental forming process spiral coordinates with a 60° forming angle

The deformed part has a major diameter of 70 mm and a total depth of 45 mm with a step down of 0.5 mm. The tool is rotationally fixed, and its feed rate is 2800 mm/min within the forming process.

5. Results of the numerical analysis of single point incremental forming

5. 1. Results of calibration and the coefficients of the Yld2000-2D function

The calculated parameters for the Voce type hardening law are outlined in Table 3.

A MATLAB code adopted the experimental values in Tables 1, 2 to predict the coefficients of Yld2000-2D outlined in Table 4.

Table 3

Predicted Voce type hardening parameters for AL20 and AL70 sheets

Material	β (MPa)	ω (MPa)	λ
AL20	278.6	98.87	27.15
AL70	73.34	161.24	26.89

Table 4

Coefficients of Yld2000-2D for AL20 and AL70

Material	k_1	k_2	k_3	k_4	k_5	k_6	k_7	k_8
AL20	0.500	1.260	0.547	1.009	1.070	0.969	1.231	1.505
AL70	1.015	0.863	0.661	0.971	0.956	0.735	0.984	1.255

Fig. 2 compares experimental normalized yield stresses and *r*-values with the values predicted by the Yld2000-2D model. The curves reveal that the Yld2000-2D model can reliably represent the planar anisotropic behavior of the yield stresses and *r*-values of the analyzed materials under uniaxial and biaxial tensile conditions.

The comparison between the von Mises and Yld2000-2D yield surfaces for AL20 and AL70 for the 2D plane stress condition in the RD-TD plane is shown in Fig. 3.

A remarkable variation between the shapes of the Yld2000-2D and von Mises yield surfaces in Fig. 3 is affected by the Al alloys anisotropy. Variations in the stress levels of the various strain paths, such as the plane strain, and the balanced biaxial conditions of the two metals can be observed.

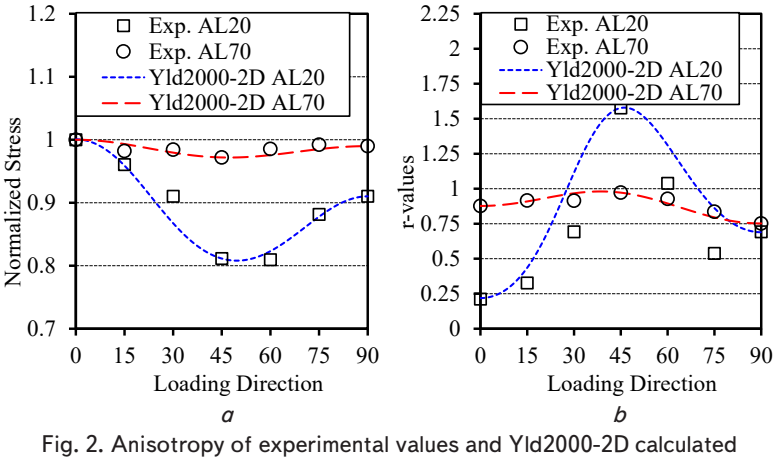

Fig. 2. Anisotropy of experimental values and Yld2000-2D calculated values of: *a* — normalized yield stress; *b* — *r*-values

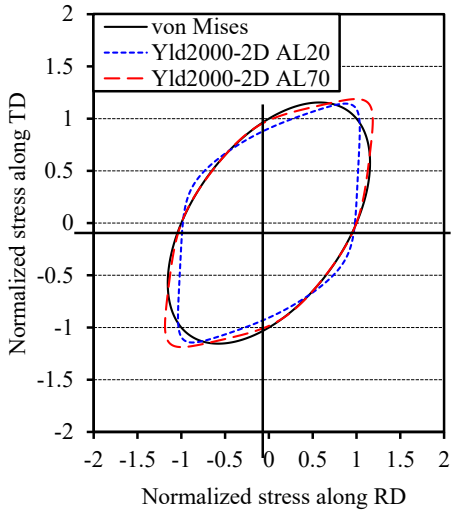

Fig. 3. Predicted von Mises and Yld2000-2D yield surfaces for plane stress condition

5. 2. Results of constructing a geometry and finite element model

The yield function was implemented by the stress integration algorithm, within the condition of rate-independent plasticity, as a user material subroutine VUMAT (FORTRAN code) within the FE software Abaqus/Explicit. Fig. 4 shows the FE model of the bilayer sheet and the forming tool applied in the SPIF simulation.

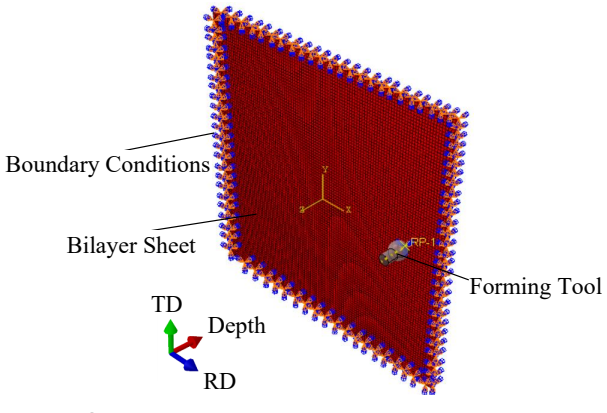

Fig. 4. Schematic of the undeformed finite element model of the bilayer sheet

According to the ABAQUS manual [15], applying the explicit dynamic procedure with Abaqus/Explicit to quasi-static problems demands careful consideration. The amount of time to simulate the SPIF process in its natural time scale can be reduced by decreasing the percentage of kinetic energy to internal energy to under 10 %. Therefore, to verify the accuracy and stability of the simulation process, a fixed mass scaling of 10^6 was used to maximize the lowest desired time increment. A preliminary study was performed, and it was found that the kinetic energy was insignificant relative to the internal energy. This demonstrates that the mass scaling factor was appropriate for the numerical implementation.

5. 3. Results of the effect of anisotropy and layer arrangement on the equivalent plastic strain, thickness variation, and reaction forces

The EPS distributions for the surfaces of the bilayer sheet for both isotropic and anisotropic behavior with different layer arrangements are shown in Fig. 5, 6. According to the comparison of the EPS distributions of the AL70/AL20 layer arrangements in Fig. 5, the highest plastic strain can be observed in the top layer, for which the tool is in contact with the AL70 sheet layer. More specifically, the stress history at the top surface is extremely dynamic and complicated due to the tool contact, which accumulates additional plastic strain. Additionally, the fluctuated bending and unbending behaviors due to the tool movement in SPIF increase the EPS on both the top and bottom surfaces, especially for the low-strength AL70 top sheet layer. The EPS distributions for the AL20/AL70 layer arrangement shown in Fig. 6 predict higher EPS values for the AL70 compared to the AL70/AL20 layer arrangements in Fig. 5.

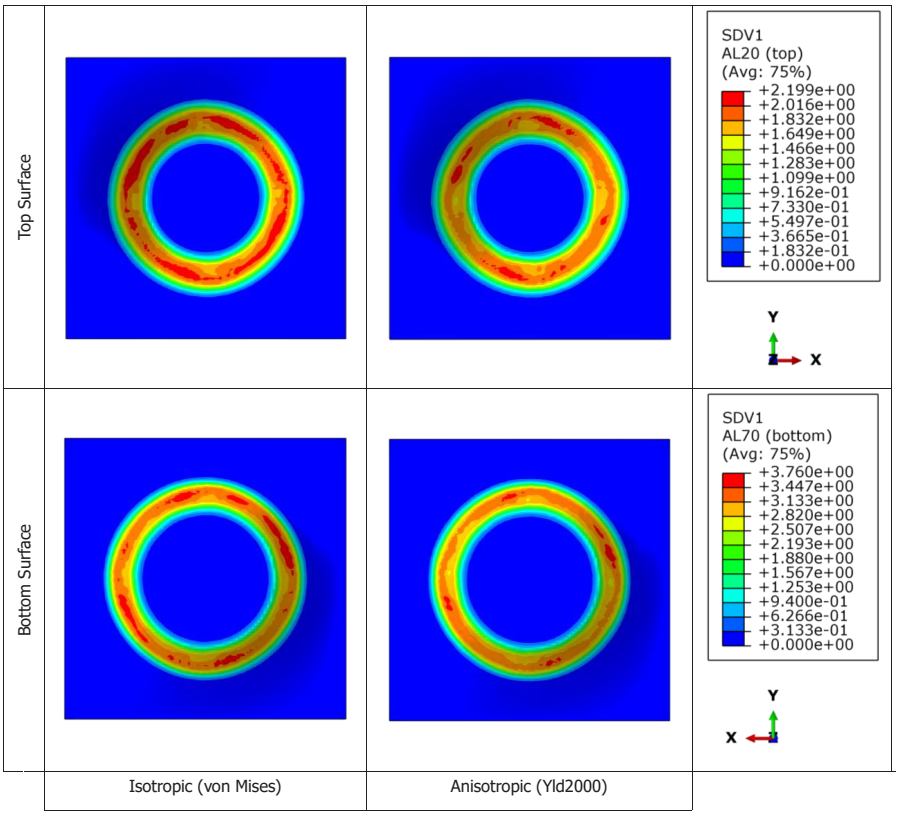

Fig. 6. Contours of the equivalent plastic strain distribution on the top and bottom surfaces of the AL20/AL70 layer sheet arrangement

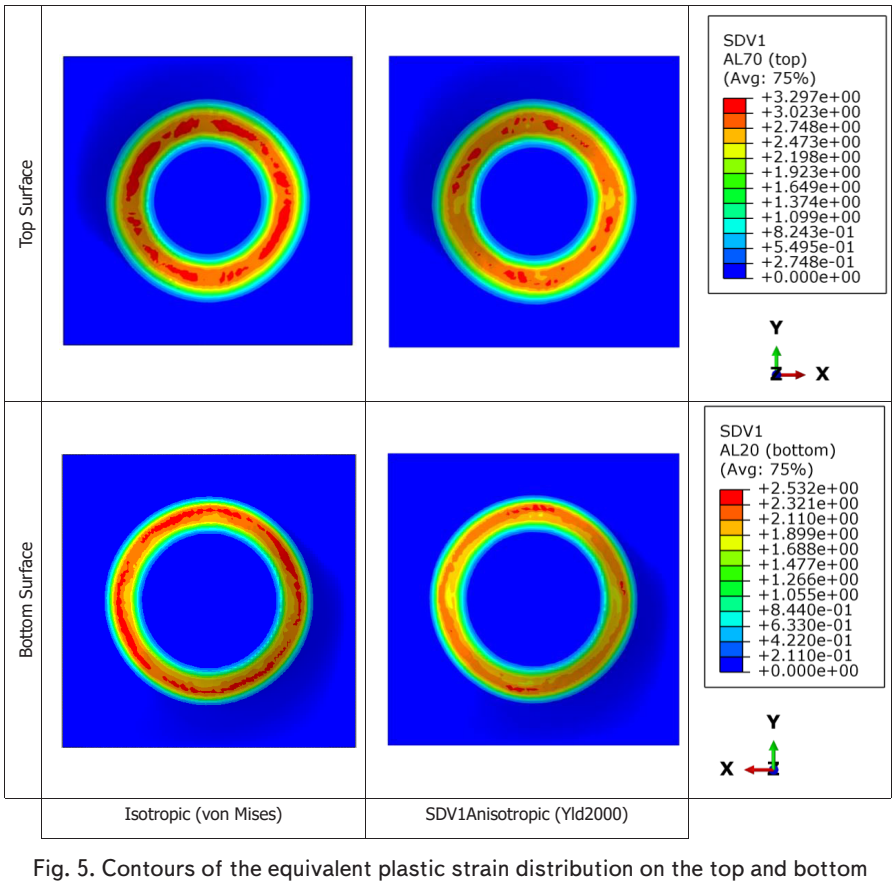

Fig. 5. Contours of the equivalent plastic strain distribution on the top and bottom surfaces of the AL70/AL20 layer sheet arrangement

The EPS for the AL20/AL70 layer arrangement increased by 0.463 for AL70 and decreased by 0.333 for AL20.

Fig. 7 shows a comparison of the thickness distribution of the part formed with SPIF. The layer arrangements and anisotropy have obvious effects on the bilayer sheet thickness. As a result of stretching, the AL70/AL20 had a smaller thickness than that predicted for the AL20/AL70 layer arrangement at a tool depth of less than 5 mm. However, for a similar formed part, the AL70 layer thickness in the AL70/AL20 layer arrangement is larger than that of AL20.

Fig. 8 compares the thickness strain variations of the AL70 and AL20 layers in both layer arrangements by considering isotropic and anisotropic effects. As shown in Fig. 8, *a*, *b*, disregarding the layer arrangements, the layer not in contact with the tool shows a smaller distribution of strain thickness when compared to that of the contact layer. Generally, in SPIF, the outer surface accomplishes additional stretching deformations compared to the inner surface.

Fig. 8, *b* shows that a higher strength layer (AL20) in the AL20/AL70 layer arrangement experiences less thickness strain compared to the AL70/AL20 layer arrangement.

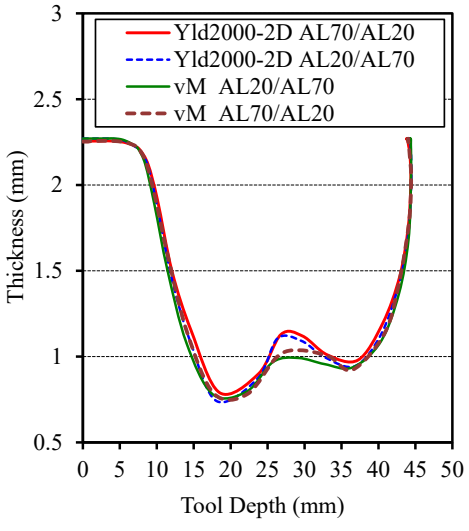

Fig. 7. Thickness variation along the rolling direction

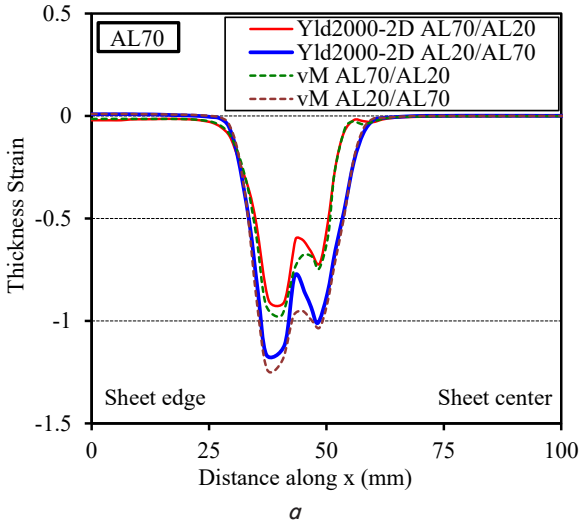

a

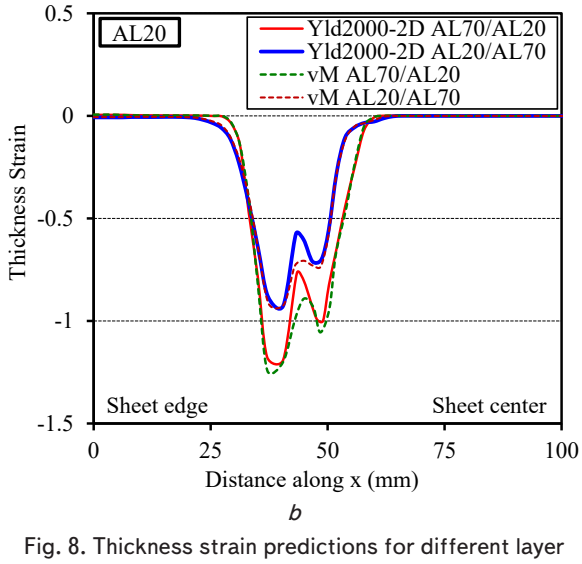

b

Fig. 8. Thickness strain predictions for different layer arrangements and anisotropy effects of: *a* – AL70 layer; *b* – AL20 layer

Indeed, the AL20 in AL70/AL20 undergoes more stretching and is less thick than the AL70 layer. This led to increases in the forming force and a more rapid initiation of yield in the AL70/AL20 layer arrangement compared to the AL20 in the AL20/AL70 layer arrangement.

Fig. 9 illustrates the reaction forces of the forming tool in the vertical (F_z) direction, comparing the effect of layer arrangement according to the von Mises and Yld2000-2D models.

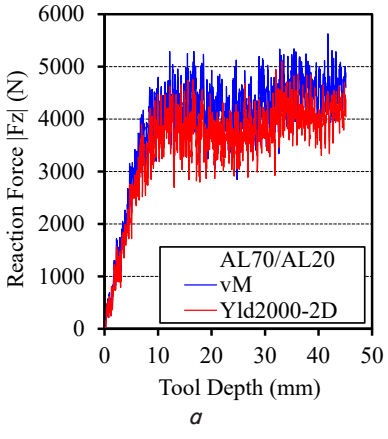

a

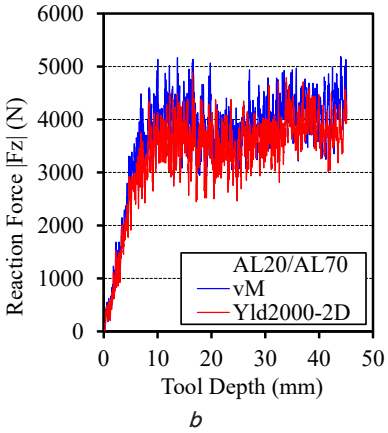

b

Fig. 9. Comparison of the vertical reaction forces (F_z) with different layer arrangements: *a* – AL70/AL20; *b* – AL20/AL70

As can be seen in Fig. 9, the vertical reaction calculated by the von Mises model predicts the vertical reactions to be larger than those predicted by the Yld2000-2D model in the case of both layer arrangements. The average vertical reaction for von Mises is 12.01 % higher than Yld2000-2D for AL70/AL20 and 9.71 % higher than Yld2000-2D for AL20/AL70.

6. Discussion of the numerical analysis results of single point incremental forming process

A comparison of the results obtained from the contours of the von Mises and Yld2000-2D models in Fig. 5, 6 shows obvious differences between the top and bottom surfaces caused by various loading paths and yield surfaces. The EPS pattern based on the Yld2000-2D model shows less strain distribution compared to the von Mises model, which is related to the shape of the yield surfaces for the AL70 and AL20 shown in Fig. 3. Most of the EPS are located between the plane strain case in the walls and the balanced biaxial tension case in the corners of the formed part. This implies that a change

in the shape of the yield surface of the aluminum sheets can have a rather significant effect on the simulated EPS.

The stronger aluminum layer (AL20) on the non-contact side of the tool, although thinner than the AL70 layer, is able to tolerate further stretching deformation than that on the contact side. The predicted measurements for bilayer thickness variation in Fig. 7 are slightly smaller for anisotropic behavior compared to isotropic behavior, especially for the AL70/AL20 layer arrangement. This analysis supports the use of the AL70/AL20 layer arrangement as it has somewhat greater formability, potentially delaying crack formation that would cause damage to both layers.

The variation of the vertical reaction of the tool in Fig. 9 between the two models is attributable to the shape of the yield surfaces under the effect of plane stress case shown in Fig. 3. The variations in the stress levels explain the variation in the forming reactions. The difference in the mechanical properties of the alloys in the bilayer sheet has a significant effect on plastic deformation in SPIF and, subsequently, on the forming forces. Therefore, the vertical force for the AL70/AL20 layer arrangement for both yield models is higher than that predicted by AL20/AL70 layer arrangements. Generally, the low yield stress for the AL70 metal leads to an earlier plastic deformation compared to the AL20 sheet metal. In the AL70/AL20 layer arrangement, when the AL70 is in contact with the tool, it starts to yield before the bottom AL20 layer, which likely undergoes additional stretching and bending when plastic deformation begins. Moreover, the additional thinning of the AL20 sheet layer in the AL70/AL20 layer arrangement contributes to increasing the vertical reaction, as compared to the AL20/AL70 layer arrangement.

The presented study considers only one type of metals (aluminum). Furthermore, it is limited to the investigation of some features of the parts formed using spiral path only with SPIF, we shall continue research in searching for a wide range of physical properties for evaluating the effect of anisotropy in SPIF with complex formed shapes.

Our findings can be further improved in the future by employing alternative advanced yield models. However, the main challenge of using advanced models is the time required to perform the simulation. Other metals with different mechanical characteristics may also be used.

The results of the research have a practical application in that they can be used to identify strategies for the anisotropic bimetal sheet to improve such material forming techniques in the industry.

7. Conclusions

1. The implemented Yld2000-2D anisotropic yield function captured the planar anisotropic behavior of the yield stresses and *r*-values of the investigated metals as compared with the experimental results. The YLD2000-2D curve closely matches the experimental data in terms of shape and tendency, especially for AL70 sheet metal. Additional parameters from extra experiments and much advanced yield criterion can be used to precisely match the experimental results of AL20 sheet metal.

2. Comparing the numerical results of the von Mises and Yld2000-2D contours for the equivalent plastic strain, there are noticeable variances between the top and bottom surfaces induced by different loading paths and yield surfaces. The Yld2000-2D model's equivalent plastic strain pattern displays less strain distribution than the von Mises model. This indicates that changing the yield surface shape of aluminum sheets can have a significant impact on the simulated EPS.

3. Anisotropic behavior predicts smaller bilayer thickness variation than isotropic behavior in the numerical simulation, particularly for the AL70/AL20 layer arrangement. Therefore, the AL70/AL20 layer arrangement has better formability and potentially delaying crack initiation that would damage both layers. The AL70/AL20 layer arrangement's reaction vertical force is higher than the AL20/AL70 layer arrangement's prediction. In general, the lower yield stress of AL70 sheet metal causes plastic deformation to occur sooner than in AL20.

References

1. Hagan, E., Jeswiet, J. (2003). A review of conventional and modern single-point sheet metal forming methods. Proceedings of the Institution of Mechanical Engineers, Part B: Journal of Engineering Manufacture, 217 (2), 213–225. doi: https://doi.org/10.1243/095440503321148858
2. Liu, Z., Li, G. (2019). Single point incremental forming of Cu-Al composite sheets: A comprehensive study on deformation behaviors. Archives of Civil and Mechanical Engineering, 19 (2), 484–502. doi: https://doi.org/10.1016/j.acme.2018.11.011
3. Zhang, Q., Guo, H., Xiao, F., Gao, L., Bondarev, A. B., Han, W. (2009). Influence of anisotropy of the magnesium alloy AZ31 sheets on warm negative incremental forming. Journal of Materials Processing Technology, 209 (15-16), 5514–5520. doi: https://doi.org/10.1016/j.jmatprotec.2009.05.012
4. Palumbo, G., Brandizzi, M., Cervelli, G., Fracchiolla, M. (2011). Investigations about the Single Point Incremental Forming of Anisotropic Titanium Alloy Sheets. Advanced Materials Research, 264-265, 188–193. doi: https://doi.org/10.4028/www.scientific.net/amr.264-265.188
5. Seong, D. Y., Haque, M. Z., Kim, J. B., Stoughton, T. B., Yoon, J. W. (2014). Suppression of necking in incremental sheet forming. International Journal of Solids and Structures, 51 (15-16), 2840–2849. doi: https://doi.org/10.1016/j.ijsolstr.2014.04.007
6. Karajibani, E., Hashemi, R., Sedighi, M. (2016). Forming limit diagram of aluminum-copper two-layer sheets: numerical simulations and experimental verifications. The International Journal of Advanced Manufacturing Technology, 90 (9-12), 2713–2722. doi: https://doi.org/10.1007/s00170-016-9585-1
7. Uscinowicz, R. (2013). Experimental identification of yield surface of Al–Cu bimetallic sheet. Composites Part B: Engineering, 55, 96–108. doi: https://doi.org/10.1016/j.compositesb.2013.06.002

8. Chen, C.-Y., Kuo, J.-C., Chen, H.-L., Hwang, W.-S. (2006). Experimental Investigation on Earing Behavior of Aluminum/Copper Bimetal Sheet. MATERIALS TRANSACTIONS, 47 (9), 2434–2443. doi: https://doi.org/10.2320/matertrans.47.2434
9. Bagherzadeh, S., Mirnia, M. J., Mollaei Dariani, B. (2015). Numerical and experimental investigations of hydro-mechanical deep drawing process of laminated aluminum/steel sheets. Journal of Manufacturing Processes, 18, 131–140. doi: https://doi.org/10.1016/j.jmapro.2015.03.004
10. von Mises, R. (1913). Mechanics of solid bodies in the plastically-deformable state. Math.-Phys. Klasse, 4. Available at: http://www.neo-classical-physics.info/uploads/3/0/6/5/3065888/von_mises_-_plastic_deformation.pdf
11. Barlat, F., Brem, J. C., Yoon, J. W., Chung, K., Dick, R. E., Lege, D. J. et. al. (2003). Plane stress yield function for aluminum alloy sheets – part 1: theory. International Journal of Plasticity, 19 (9), 1297–1319. doi: https://doi.org/10.1016/s0749-6419(02)00019-0
12. Simo, J. C., Hughes, T. J. R. (1998). Computational Inelasticity. Springer, 392. doi: https://doi.org/10.1007/b98904
13. Chung, K., Lee, S. Y., Barlat, F., Keum, Y. T., Park, J. M. (1996). Finite element simulation of sheet forming based on a planar anisotropic strain-rate potential. International Journal of Plasticity, 12 (1), 93–115. doi: https://doi.org/10.1016/s0749-6419(95)00046-1
14. Leacock, A. G., Howe, C., Brown, D., Lademo, O.-G., Deering, A. (2013). Evolution of mechanical properties in a 7075 Al-alloy subject to natural ageing. Materials & Design, 49, 160–167. doi: https://doi.org/10.1016/j.matdes.2013.02.023
15. Abaqus 6.14. Available at: http://130.149.89.49:2080/v6.14/